On the Ability of Modified Peptide Links to Form Hydrogen Bonds

Carlos Alemán*

Departament d'Enginyeria Química, E.T.S. d'Enginyers Industrials de Barcelona, Universitat Politécnica de Catalunya, Diagonal 647, Barcelona E-08028, Spain

Received: January 17, 2001; In Final Form: April 11, 2001

The hydrogen-bonding capabilities of modified amide groups have been investigated by theoretical methods. More specifically, the groups considered in this work are retroamide, *N*-hydroxamide, *N*-amino amide, and thioamide, which are usually employed to design pseudopeptides. Ab initio calculations with inclusion of correlation effects at the Møller−Plesset level have been used to characterize complexes containing the interaction between a standard amide group and a modified amide group. Furthermore, self-consistent reaction-field calculations have been performed to analyze the effects of the aqueous solvent on these complexes. The results allow rationalization of the changes induced in the hydrogen-bonding network by modification of the amide bond.

Introduction

Modified amino acid residues have been used to design both peptides and peptidomimetics with a controlled fold in the backbone.[1] Among the strategies employed to modify amino acid residues is the alteration of the peptide bond.[2,3] Thus, the introduction of modified peptide links makes possible influencing the biological properties of a molecule but retaining the receptor binding ability, which usually depends of the side chains.[3,4] Another potential advantage is that compounds with modified peptide links, which are denoted pseudopeptides, are less biodegradable than native peptides.[3,4]

The most common modified amide bonds are retroamide, *N*-hydroxamide, *N*-amino amide, and thioamide, which are schematically displayed in Figure 1. The crystal structure of pseudopeptide models have revealed that their dimensions are similar to those of the standard peptide bonds and that all are found in trans planar conformation.[4−6] Nevertheless, modification of peptide bonds usually induces important conformational changes. This is because important alterations in the intra- and intermolecular hydrogen-bonding networks are produced. A large number of studies about the properties of peptide bond itself and the amide hydrogen bond formation have been reported in the last years.[7] Conversely, the interactions formed by modified amide bonds have received little attention.[4−6]

In this work, a quantum mechanical study of the interactions between an amide bond and a modified amide bond is presented. For this purpose, ab initio methods with inclusion of electron correlation effects have been used. Hydrogen-bonding energies have been estimated considering the following modified amide bonds: retroamide, *N*-hydroxamide, *N*-amino amide, and thioamide. Furthermore, self-consistent reaction-field (SCRF) calculations in aqueous solution have been performed to gain insight into the effect of the bulk solvent on the hydrogen-bonding interactions.

Methods

Model molecules containing the functional groups displayed in Figure 1 were built by adding methyl groups at the ends. The resulting compounds were $CH_3NHCOCH_3$, *N*-CH_3-$NOHCOCH_3$, $CH_3NNH_2COCH_3$, and $CH_3NHCSCH_3$. To examine the interaction between the amide bond and each modified bond, we considered bimolecular complexes constituted by these model molecules.

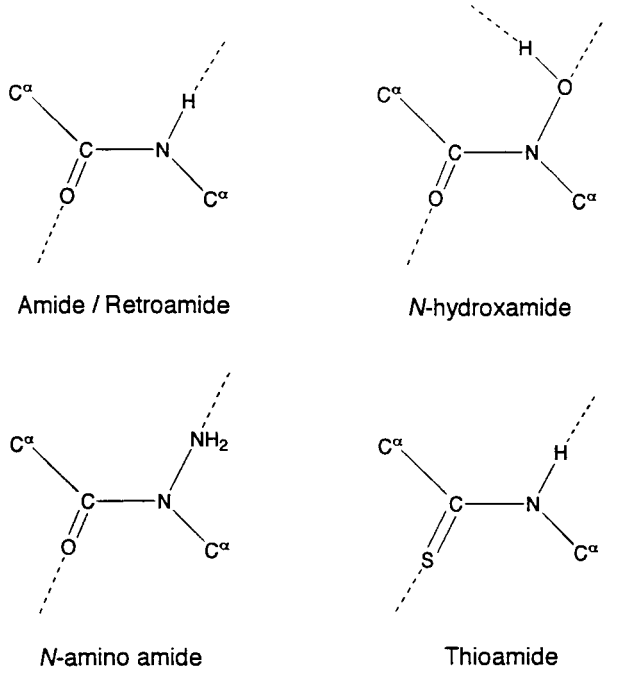

Figure 1. Modified amide groups investigated in this work. The hydrogen-bonding schemes are indicated by dashed lines.

Calculations were performed using the Gaussian 98 Rev. A7 program.[8] The structures of both complexes and isolated monomers were determined in the gas-phase by full geometry optimizations at the second-order Møller−Plesset (MP2) level[9] with the 6-31G(d) basis set.[10] Single-point energy calculations were performed on the MP2/6-31G(d) geometries at both the HF/6-311G(d,p)[11] and MP2/6-311G(d,p) levels. The counterpoise (CP) correction method was applied to correct the basis set superposition error (BSSE).[12] The interaction energy in the gas phase ($E_{Int,g}$)was calculated according to eq 1

$$E_{Int,g} = E_{ab} - E_{a,comp} - E_{b,comp} \quad (1)$$

10.1021/jp010198p CCC: $20.00
Published on Web 06/19/2001

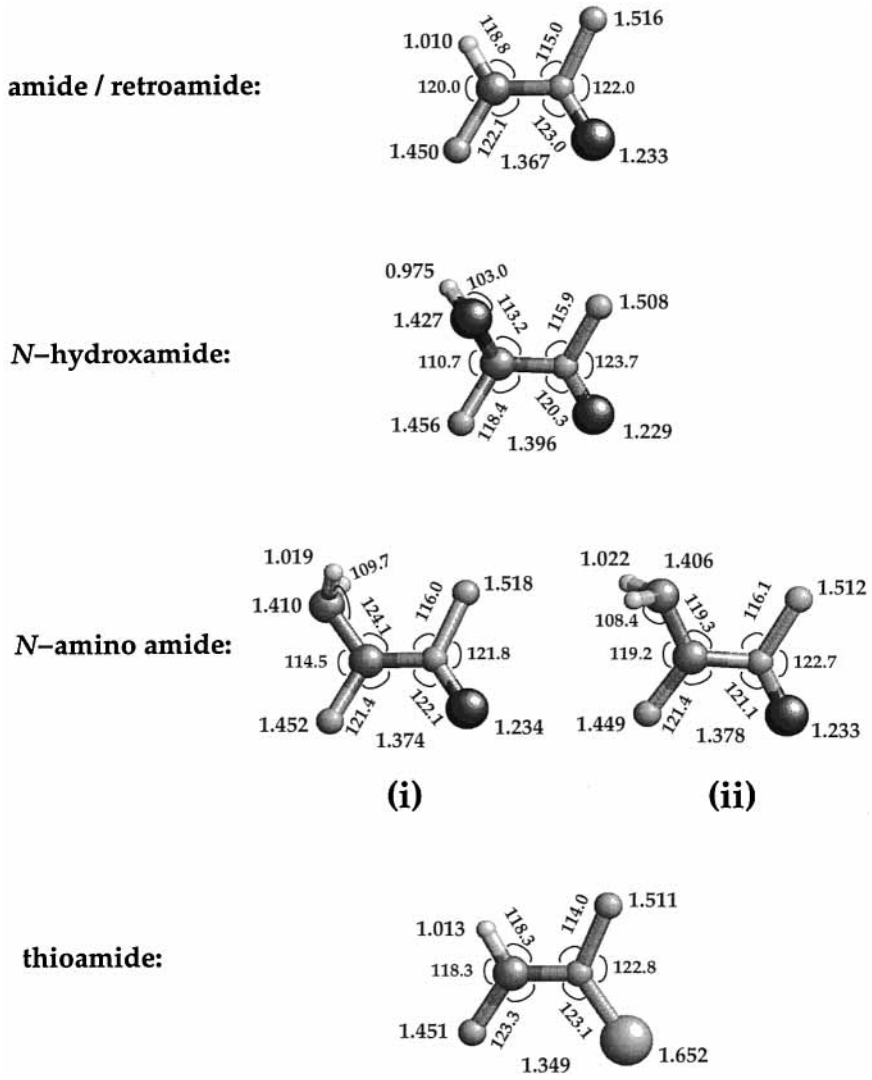

Figure 2. Molecular geometries of the amide/retromide, *N*-hydroxymide, *N*-amino amide, and thioamide groups obtained from MP2/6-31G(d) geometry optimizations. Bond lengths and bond angles are in Å and deg, respectively. Hydrogen atoms of the end methyl groups have been omitted.

where E_{ab} corresponds to the total energy of the optimized complex and $E_{a,comp}$ and $E_{b,comp}$ are the energies of the isolated monomers with the geometries obtained from the optimization of the complex.

The distortion energy (E_{Dis}), which estimates the relaxation of the monomers on dimer formation, was computed by using eq 2

$$E_{Dis} = (E_{a,comp} + E_{b,comp}) - (E_{a,opt} - E_{b,opt}) \quad (2)$$

where $E_{a,opt}$ and $E_{b,opt}$ are the energies obtained from the optimization of the isolated monomers. Thus, the net binding energies in the gas phase ($E_{Bind,g}$) were evaluated as the interaction energy in the gas phase minus the distortion energy

$$E_{Bind,g} = E_{Int,g} - E_{Dis} \quad (3)$$

The effect of the aqueous solvent on the interaction energies was estimated following the polarizable continuum model (PCM) developed by Miertus, Scrocco and Tomasi.[13] PCM calculations were performed in the framework of the ab initio HF level with the 6-311G(d,p) basis set and using the gas-phase optimized geometries. Thus, solvent-induced changes in bond lengths and angles are expected to have little influence on the free energies of solvation (ΔG_{sol}).[14] The interaction energy in aqueous solution ($E_{Int,aq}$) was evaluated by using eq 4

$$E_{Int,aq} = E_{Int,g} + \Delta\Delta G_{assoc} \quad (4)$$

where $\Delta\Delta G_{assoc}$ is the difference between the free energy of solvation of the complex ($\Delta G_{sol,ab}$) and the separated monomers ($\Delta G_{sol,a}$ and $\Delta G_{sol,b}$)

$$\Delta\Delta G_{assoc} = \Delta G_{sol,ab} - \Delta G_{sol,a} - \Delta G_{sol,b} \quad (5)$$

All calculations were performed on a IBM/SP2 at the Centre de Supercomputació de Catalunya (CESCA).

Results and Discussion

Molecular Geometries of the Modified Amide Bonds. The most relevant geometric trends of the amide/retroamide, *N*-hydroxamide, *N*-amino amide, and thioamide groups, which where obtained from geometry optimizations of the model molecules at the MP2/6-31G(d) level, are displayed in Figure 2.

Some dimensions of the *N*-hydroxamide group differ from those of the standard peptide group. The most important ones are the N−CO bond length, which is about 0.03 Å larger in the former than in the latter, and the bond angles around the nitrogen

TABLE 1: Free Energies of Solvation (ΔG_{Sol}, in kcal/mol), Gas-Phase and Aqueous Phase Dipole Moments (μ_g and μ_{Aq}, in Debyes), and Solvent-Induced Dipole Factor (μ_{Aq}/μ_g) for the Amide, *N*-hydroxamide, *N*-amino Amide, and Thioamide Groups[a]

group	ΔG_{sol}	μ_g	μ_{aq}	μ_{aq}/μ_g
amide	−9.4	4.12	5.41	1.31
N-hydroxamide	−8.7	3.39	4.28	1.26
N-amino amide[b]	−10.6	3.91	5.12	1.31
	−9.9	4.45	5.76	1.29
thioamide	−7.6	5.25	7.06	1.34

[a] Free energies of solvation and aqueous-phase dipole moments were derived from the PCM/6-311G(d,p) calculations on the following model molecules: $CH_3NHCOCH_3$, $CH_3NOHCOCH_3$, $CH_3NNH_2COCH_3$, and $CH_3NHCSCH_3$. [b] Results correspond to the top and bottom arrangements displayed in Figure 2 for the *N*-amino amide group.

atom. Thus, the *N*-hydroxamide group presents pyramidality in this atom, whereas a planar geometry is adopted in the amide group. The planar or pyramidal geometry is usually represented by the sum of the three bond angles around the nitrogen ($\Sigma\angle$XNX). Thus, a value of $\Sigma\angle$XNX closer to 360° indicates a greater degree of planarity. The values of $\Sigma\angle$XNX for the amide and *N*-hydroxamide links are 360.9° and 342.3°, respectively, indicating a degree of puckering in the latter. Other interesting features of the *N*-hydroxamide group are the sp^3 character of the hydroxyl oxygen, denoted by both bond lengths and angles involving this atom, and the orientation of O−H bond, which is almost perpendicular to the amide plane.

It is worth noting that the dimensions of the *N*-amino amide link are very similar to those of the amide group. This is especially remarkable in bond lengths and angles around the carbonyl group and in the planar geometry of the nitrogen atom ($\Sigma\angle$XNX = 360.0°). However, the most relevant characteristic of the *N*-amino amide group is that the *N*-amino moiety can present two different orientations with respect to the amide plane. As can be seen in Figure 2, in these arrangements the hydrogen atoms (i) or the lone pair (ii) are in front of the α-carbon atom. Although the dimensions of the *N*-amino amide group are very similar in both arrangements, i.e., the main differences occur in the angles around the nitrogen atom, the latter is 2.8 and 2.1 kcal/mol more stable than the former at the HF/6-311G(d,p)//MP2/6-31G(d) and MP2/6-311G(d,p)//MP2/6-31G(d) levels, respectively.

Figure 2 indicates that replacement of the carbonyl oxygen in the amide group by a sulfur atom resulted in small changes in bond lengths and angles. Thus, the most important differences betweem the thioamide and amide groups are (i) the N−CS bond length, which is about 0.02 Å shorter in the former, and (ii) the C═S bond length being 0.419 Å larger than the C═O one.

Solvation of the Modified Amide Bonds. The free energy of solvation for each model molecule determined from PCM/6-311G(d,p) calculations is given in Table 1. Results indicate that the *N*-amino amide is the best solvated group. Moreover, the arrangement with the hydrogen atoms in front of the α-carbon is 0.7 kcal/mol better hydrated than the arrangement in which the α-carbon atom is confronted to the lone pair. The solvation of the amide, *N*-hydroxamide and thiamide groups is less favored by 1.2, 1.9, and 3 kcal/mol.

Table 1 includes the solution-phase and gas-phase dipole moments (μ_g and μ_{aq}, respectively), which have been used to investigate the magnitude of the polarization effects provided by the solvent. This has been estimated by determining the solvent induced dipole factor (μ_{aq}/μ_g). Results indicate that the increase of dipole moment in water with respect to that in the gas phase ranges from 26% (*N*-hydroxamide) to 34% (thioamide). It is worth noting that the large dipole moment of the thioamide group does not provide the most favorable interaction with the solvent. Indeed, the solvation energies displayed in Table 1 cannot be explained in terms of molecular dipole moments. Conversely, there is good correlation between the solvation free energies and the partial atomic charges. Table 2 lists the atomic charges determined from HF/6-311G(d,p) molecular electrostatic potentials for the amide/retroamide, *N*-hydroxamide, *N*-amino amide, and thioamide groups.[15] As can be seen, the free energy of solvation becomes more favorable when the magnitude of the partial charges associated with the solvent-exposed atoms increases.

TABLE 2: Partial Atomic Charges (in units of electron) for the Amide, *N*-hydroxamide, *N*-amino Amide, and Thioamide Groups[a]

amide		N-hydroxamide		N-amino amide		thioamide	
N	−0.519	N	−0.296	N	0.131	N	−0.199
H	0.321	O(−N)	−0.464	N(−N)	−0.874	H	0.269
C	0.781	H	0.426	H	0.378	C	0.280
O	−0.615	C	0.883	C	0.693	S	−0.429
		O(═C)	−0.617	O	−0.646		

[a] Charges derived from the HF/6-311G(d,p) molecular electrostatic potentials considering the following model molecules: $CH_3NHCOCH_3$, $CH_3NOHCOCH_3$, $CH_3NNH_2COCH_3$, and $CH_3NHCSCH_3$.

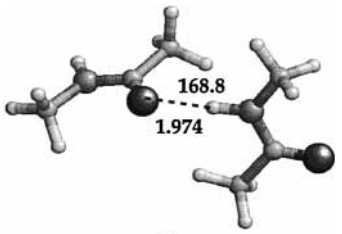

I

Figure 3. Optimized geometry of the bimolecular complex **I** ($CH_3NHCOCH_3$...$CH_3NHCOCH_3$) from MP2/6-31G(d) calculations. The hydrogen...acceptor distance (in Å) and donor-hydrogen...acceptor angle (in deg) are indicated.

Hydrogen-Bonding Interactions in the Gas-Phase. The 11 complexes investigated in the present work are displayed in Figures 3−8. The interaction energies (eq 1) computed correcting and without correcting the BSSE are listed in Table 3, whereas the distortion (eq 2) and binding energies (eq 3) are displayed in Table 4. The relative energies among the different complexes computed for two given monomers are reported in Table 5.

Table 3 indicates that the BSSE plays a very important role in both HF/6-311G(d,p)//MP2/6-31G(d) and MP2/6-311G(d,p)//MP2/6-31G(d) calculations. However, its magnitude shows a dependence on the complex subject of study. Thus, the contribution of the BSSE to the interaction energy ranges from 25−35% (HF to MP2) for complex **I** to 45−55% (MP2 to HF) for complex **IIb**. It should be mentioned the CP is the most used method to correct the BSSE, even though its usefulness has been controversial. Thus, there is a widespread feeling that the values of the BSSE obtained by the CP method are only approximate and that this method overestimates the size of the BSSE.[16] On the other hand, as can be seen in Tables 3 and 4, the inclusion of electron correlation at the MP2 level leads to more favorable interaction and binding energies, which are enlarged by around 0.7−3.7 kcal/mol compared to the HF results. The increase in the interaction and binding energies upon treatment of electron correlation effects has been previously reported for other hydrogen-bonded complexes.[17]

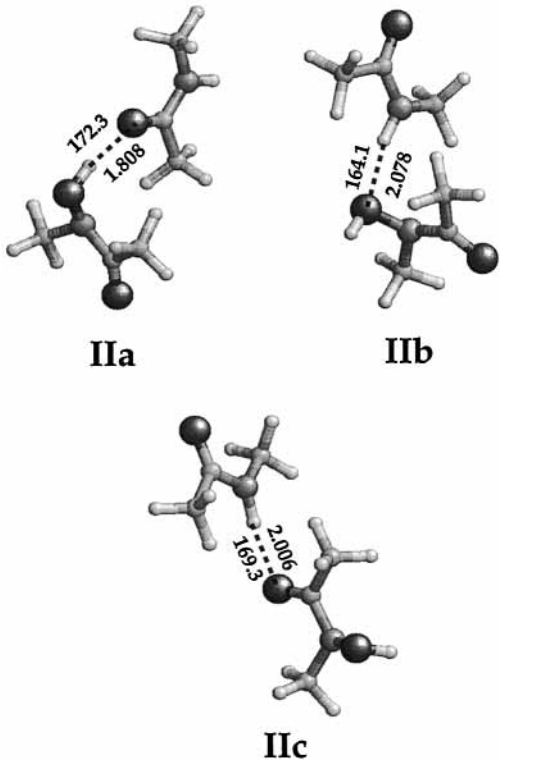

Figure 4. Optimized geometries of the bimolecular complexes **II** ($CH_3NHCOCH_3$...$CH_3NOHCOCH_3$) from MP2/6-31G(d) calculations. The hydrogen...acceptor distances (in Å) and donor-hydrogen...acceptor angles (in deg) are indicated.

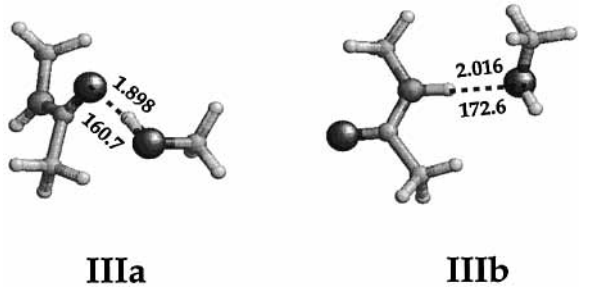

Figure 5. Optimized geometries of the bimolecular complexes **III** ($CH_3NHCOCH_3$...CH_3OH) from MP2/6-31G(d) calculations. The hydrogen...acceptor distances (in Å) and donor-hydrogen...acceptor angles (in deg) are indicated.

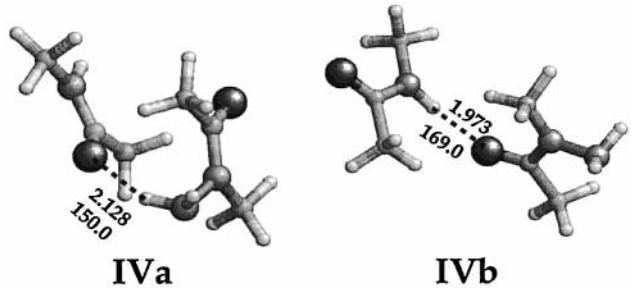

Figure 6. Optimized geometries of the bimolecular complexes **IV** ($CH_3NHCOCH_3$...$CH_3NNH_2COCH_3$) from MP2/6-31G(d) calculations. The hydrogen...acceptor distances (in Å) and donor-hydrogen...acceptor angles (in deg) are indicated.

Amide...Amide/Retroamide. The structure of the bimolecular complex $CH_3NHCOCH_3$...$CH_3NHCOCH_3$ (**I**) resulting from complete geometry optimization at the MP2/6-31G(d) level is displayed in Figure 3. The interaction energy at the MP2/6-311G(d,p) level of theory is −6.6 kcal/mol. This value is in excellent agreement with other values reported in the literature: −6.6 kcal/mol was calculated using the DGauss density functional theory program with the DZPV2 basis set,[7h] and −6.9 and −6.8 kcal/mol were calculated at the MP2/cc-pVTZ[7h] and HF/6-31G(d)[7f] levels, respectively. The binding energy indicates that the changes in the molecular geometries of the monomers after the complexation are quite small, the distortion energy being lower than 1 kcal/mol.

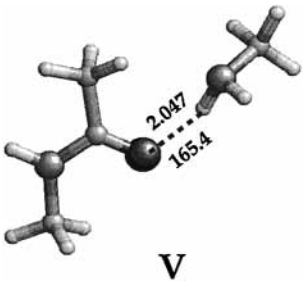

Figure 7. Optimized geometry of the bimolecular complex **V** ($CH_3NHCOCH_3$...CH_3NH_2) from MP2/6-31G(d) calculations. The hydrogen...acceptor distance (in Å) and donor-hydrogen...acceptor angle (in deg) are indicated.

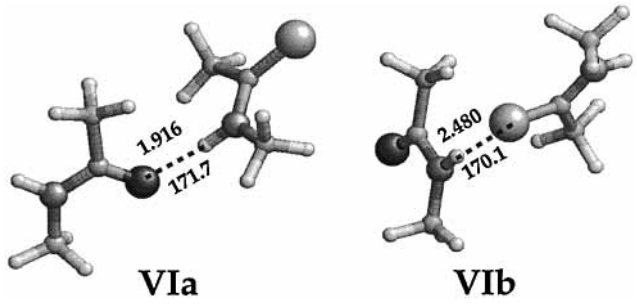

Figure 8. Optimized geometries of the bimolecular complexes **VI** ($CH_3NHCOCH_3$...$CH_3NHCSCH_3$) from MP2/6-31G(d) calculations. The hydrogen...acceptor distances (in Å) and donor-hydrogen...acceptor angles (in deg) are indicated.

Amide...N-Hydroxamide. Full geometry optimization of the bimolecular complex $CH_3NHCOCH_3$...$CH_3NOHCOCH_3$ in various geometrical arrangements led to three minimum-energy structures (**IIa**, **IIb**, and **IIc**). The optimized geometries and intermolecular parameters are displayed in Figure 4. Complex **IIa** presents a hydrogen bond between the oxygen atom of the amide group and the hydroxyl hydrogen of the *N*-hydroxamide group. On the other hand, complexes **IIb** and **IIc** involve interactions between the amide hydrogen and the hydroxyl and carbonyl oxygen atoms of the *N*-hydroxamide group, respectively.

The relative energy obtained for the different complexes is **IIa** > **IIc** > **IIb** (Table 5), the interaction energies ranging from −4.1 to −10.0 kcal/mol at the MP2/6-311G(d,p)//MP2/6-31G(d) level (Table 3). These results clearly show that the hydrogen of the *N*-hydroxamide group provides a strong interaction with the amide oxygen atom (complex **IIa**). Indeed, the interaction energy of this complex is about 3.3 kcal/mol larger than that that predicted for the amide hydrogen bond in complex **I**. On the other hand, the hydroxyl oxygen is worse as a hydrogen acceptor than the carbonyl oxygen. Thus, the interaction energy of **IIb** is less favorable than that of **IIc** by about 2.9 and 1.6 kcal/mol at the HF/6-311G(d,p)//MP2/6-31G(d) and MP2/6-311G(d,p)//MP2/6-31G(d) levels, respectively.

The strength as proton donor predicted for the *N*-hydroxamide group is in good agreement with experimental data. Thus, IR absorption spectroscopy results revealed a stronger hydrogen

TABLE 3: Interaction Energies in the Gas Phase ($E_{Int,g}$, in kcal/mol) Computed Correcting and without Correcting the BSSE Error for the Different Complexes Investigated in This Work:[a] $CH_3NHCOCH_3$...$CH_3NHCOCH_3$ (I), $CH_3NHCOCH_3$...$CH_3NOHCOCH_3$ (II), $CH_3NHCOCH_3$...CH_3OH (III), $CH_3NHCOMe$...$CH_3NNH_2COCH_3$ (IV), $CH_3NHCOMe$...CH_3NH_2 (V), and $CH_3NHCOCH_3$...$CH_3NHCSCH_3$ (VI)

	without correcting BSSE		correcting the BSSE	
complex	HF/6-311G(d,p)	MP2/6-311G(d,p)	HF/6-311G(d,p)	MP2/6-311G(d,p)
I	−7.2	−10.4	−5.4	−6.6
IIa	−10.5	−14.0	−8.5	−10.0
IIb	−2.9	−7.3	−1.3	−4.1
IIc	−6.2	−9.6	−4.2	−5.8
IIIa	−7.8	−10.7	−5.3	−6.0
IIIb	−4.6	−5.0	−3.0	−4.4
IVa	−7.4	−12.7	−5.1	−8.2
IVb	−7.0	−10.2	−5.0	−6.6
V	−4.4	−7.0	−2.7	−3.8
VIa	−8.5	−120.0	−6.4	−8.2
VIb	−3.2	−8.3	−2.0	−4.9

[a] Complexes were optimized at the MP2/6-31G(d) level. Interaction energies were obtained from single-point calculations at the HF/6-311G(d,p) and MP2/6-311G(d,p) levels on the optimized compounds.

TABLE 4: Distortion and Binding Energies (E_{Dis} and E_{Bind}, respectively, in kcal/mol) Computed in the Gas Phase for the Different Complexes Investigated in This Work:[a] $CH_3NHCOCH_3$...$CH_3NHCOCH_3$ (I), $CH_3NHCOCH_3$...$CH_3NOHCOCH_3$ (II), $CH_3NHCOCH_3$...CH_3OH (III), $CH_3NHCOMe$...$CH_3NNH_2COCH_3$ (IV), $CH_3NHCOMe$...CH_3NH_2 (V), and $CH_3NHCOCH_3$...$CH_3NHCSCH_3$ (VI)

	HF/6-311G(d,p)		MP2/6-311G(d,p)	
complex	E_{Dis}	E_{Bind}[b]	E_{Dis}	E_{Bind}[b]
I	0.9	−4.5	0.7	−5.9
IIa	1.8	−6.7	1.2	−8.8
IIb	2.6	1.3	2.5	−1.6
IIc	0.6	−3.5	0.5	−5.3
IIIa	0.9	−4.3	0.6	−5.5
IIIb	0.4	−2.6	0.3	−4.1
IVa	1.7	−3.4	1.1	−7.1
IVb	0.7	−4.3	0.5	−6.0
V	0.4	−2.3	0.3	−3.5
VIa	0.8	−5.6	0.7	7.4
VIb	0.4	−1.6	0.3	−4.6

[a] Complexes were optimized at the MP2/6-31G(d) level. E_{Dis} and E_{Bind} were obtained from single-point calculations at the HF/6-311G(d,p) and MP2/6-311G(d,p) levels on the optimized compounds. [b] Computed using the interaction energies corrected with the counterpoise method.

TABLE 5: Energy[a] (E, in au) and Energy Difference[b] (ΔE, in kcal/mol) Computed in the Gas Phase for the Different Complexes Investigated in This Work: $CH_3NHCOCH_3$...$CH_3NHCOCH_3$ (I), $CH_3NHCOCH_3$...$CH_3NOHCOCH_3$ (II), $CH_3NHCOCH_3$...CH_3OH (III), $CH_3NHCOMe$...$CH_3NNH_2COCH_3$ (IV), $CH_3NHCOMe$...CH_3NH_2 (V), and $CH_3NHCOCH_3$...$CH_3NHCSCH_3$ (VI)

	HF/6-311G(d,p)		MP2/6-311G(d,p)	
complex	E	ΔE	E	ΔE
I	−494.149758	-	−495.783261	-
IIa	−568.968235	0.0	−570.802125	0.0
IIb	−568.954843	8.4	−570.789453	7.9
IIc	−568.963132	3.2	−570.796189	3.7
IIIa	−362.154915	0.0	−563.336279	0.0
IIIb	−362.150686	2.6	−363.331266	3.1
IVa	−549.149883	3.4	−550.968886	0.1
IVb	−549.155254	0.0	−550.969120	0.0
V	−342.317937	-	−343.481936	-
VIa	−816.788550	0.0	−818.360199	0.0
VIb	−816.781148	4.6	−818.354898	3.3

[a] Complexes were optimized at the MP2/6-31G(d) level. Energies were estimated from single-point calculations at the HF/6-311G(d,p) and MP2/6-311G(d,p) levels. [b] Energy differences within each complex are computed with respect to the most stable arrangement.

bond in compounds involving a *N*-hydroxamide group than in compounds with nonmodified amide bonds.[4,5] Thus, the *N*-hydroxamide group was found to be a strong proton donor capable of very short contacts with carbonyl oxygen atoms.

On the other hand, the strength of the hydrogen bonds involved in complexes **I**, **IIa**, **IIb**, and **IIc** is consistent with the atomic partial charges determined from molecular electrostatic potentials, which are given in Table 2. The charge of the hydroxyl hydrogen atom in the *N*-hydroxamide group is 0.10 units of electron more positive than the value of the amide hydrogen. As a result, the interaction in complex **IIa** is stronger than that in complex **I.** On the other hand, the atomic charge of the hydroxyl oxygen atom is 0.15 units of electron less negative than the charge of the amide oxygen. This is consistent with the energetic destabilization of **IIb** with respect to **IIc**.

The energy cost due to geometry distortion arising upon dimerization clearly depends on the complex (Table 4). It is around 0.5 kcal/mol for complex **IIc**, whereas complexes **IIa** and **IIb** present larger distortion energies which give a measure of the large deformability of the N−OH moiety with respect to the C═O one. Thus, distortion energies of 1.2 and 2.5 kcal/mol were obtained at the MP2/6-311G(d,p)//MP2/6-31G(d) level for complexes **IIa** and **IIb**, respectively. Such large energies are due to structural changes in the *N*-hydroxamide group caused by the intermolecular interaction. Comparison between the geometrical parameters of the *N*-hydroxamide group in complexes **IIa** and **IIb** with respect those displayed in Figure 2 reveals some changes in the N−O and O−H bond lengths (∼0.01 Å) and in the ∠N−O−H bond angle (∼4°). Furthermore, important changes are also detected in the bond angles around the nitrogen atom of complex **IIb**. Thus, the value of ΣXNX changes from 342.3° for an isolated *N*-hydroxamide group to 350.1° for **IIb**. It is worth noting that in all cases (Σ∠XNX = 345.1° and 346.1° for **IIa** and **IIc**, respectively) the planarity of the *N*-hydroxamide group increases upon dimerization.

To compare the hydrogen bonds formed by the hydroxyl of the *N*-hydroxamide group with those of a classical hydroxyl group, we have examined different geometrical arrangements of the complex $CH_3NHCOCH_3$...CH_3OH (**IIIa** and **IIIb**). Figure 5 shows the structures of **IIIa** and **IIIb** optimized at the MP2/6-31G(d) level. In complex **IIIa**, the hydroxyl group donates the hydrogen to the hydrogen bond, whereas in **IIIb**, the oxygen

atom of methanol accepts the hydrogen. Thus, these complexes are closely related with **IIa** and **IIb**, respectively.

Complex **IIIa** is 3.1 kcal/mol more stable than complex **IIIb** (Table 5), an energy difference lower than that obtained between **IIa** and **IIb**. Furthermore, the interaction energy of **IIIa** is −6.0 kcal/mol, indicating that the hydrogen atom of the standard hydroxyl group provides weaker hydrogen bonds than the hydrogen atom of the *N*-hydroxamide group. On the other hand, the interaction energy of **IIIb** is 4.4 kcal/mol, which is similar to that computed for **IIb**. Thus, the oxygen atoms of the hydroxyl and *N*-hydroxamide groups do not present significant differences when they act as hydrogen acceptors.

Amide...N-Amino Amide. The two minimum-energy structures found for the bimolecular complex $CH_3NHCOCH_3...CH_3NNH_2COCH_3$ (**IVa** and **IVb**) are displayed in Figure 6. Complex **IVa** presents a hydrogen bond between the carbonyl oxygen of the amide group and one of the *N*-amino hydrogen atoms. The interaction and binding energies of this complex at the MP2/6-311G(d,p)//MP2/6-31G(d) level are −8.2 and −7.1 kcal/mol, respectively. These values are about 1.2−1.6 kcal/mol larger than those predicted for the amide...amide hydrogen bond and 1.8 kcal/mol lower than those predicted for the amide...*N*-hydroxamide interaction. Accordingly, the substitution of the amide hydrogen atom by amino and hydroxyl moieties produces stronger hydrogen bonds when the *N*-amino amide and *N*-hydroxamide groups act as hydrogen donors. However, the increase of the interaction and binding energies is larger in the latter group than in the former one. These results are in excellent agreement with experimental data. Thus, comparison of the *N*-amino and *N*-hydroxy analogues of the Piv-Pro-Gly-NHiPr peptide revealed that the *N*-amino amide group is a weaker proton donor than the *N*-hydroxamide group.[5]

In complex **IVb**, the oxygen atom of the *N*-amino amide group interacts with the amide hydrogen. As can be seen in Table 5, complex **IVb** is 3.4 kcal/mol more stable than complex **IVa** at the HF/6-311G(d,p)//MP2/6-31G(d) level, both of them becoming almost isoenergetic at the MP2/6-311G(d,p)//MP2/6-31G(d) level. Conversely, the interaction and binding energies at the latter level are 1.6 and 1.1 kcal/mol less favorable for **IVb** than for **IVa**, respectively. The distortion contribution, which is mainly associated with the *N*-amino amide link, reduces the difference between the two complexes by 0.5 kcal/mol. Nevertheless, the favorable hydrogen-bonding parameters (Figure 6) and the distortion energy are not enough to stabilize complex **IVa** with respect to complex **IVb**. The origin of such stabilization lies in the orientation of the *N*-amino hydrogen atoms in the $CH_3NNH_2COCH_3$ molecule. Thus, in complex **IVa**, the *N*-amino hydrogen atoms point to the methyl group attached to the carbonyl carbon atom (arrangement i in Figure 2), while in complex **IVb**, these hydrogen atoms are oriented toward the methyl group attached to the nitrogen (arrangement ii in Figure 2). The arrangement of the *N*-amino group in the $CH_3NNH_2COCH_3$ molecule is 2.8 and 2.1 kcal/mol more stable in **IVb** than that in **IVa** at the HF/6-311G(d,p)//MP2/6-31G(d) and MP2/6-311G(d,p)//MP2/6-31G(d) levels, respectively.

The hydrogen-bonding capabilities of the *N*-amino amide group have been compared with those of a classical amino group by examining the complex $CH_3NHCOCH_3...CH_3NH_2$ (**V**). In the optimized complex (Figure 7), the carbonyl oxygen atom interacts with the amino group. It is worth noting that the interaction with the classical amino group is weaker than the interaction with the *N*-amino amide group. Thus, the interaction and binding energies of **V** are −3.8 and −3.5 kcal/mol at the MP2/6-311G(d,p)//MP2/6-31G(d) level, which are 4.4 and 3.6 kcal/mol lower than those predicted for complex **IVa**, respectively. The higher binding capability of the *N*-amino moiety with respect to the simple amino group can be explained by the larger concentration of positive charge in the *N*-amino moiety.

TABLE 6: Free Energy of Solvation[a] (ΔG_{Sol}, in kcal/mol), Difference between the Free Energy of Solvation of the Complex and the Isolated Monomers ($\Delta\Delta G_{Assoc}$, in kcal/mol), Interaction Energy in Aqueous Solution ($E_{Int,Aq}$, in Kcal/Mol), and Energy Difference with Respect to the Most Stable Arrangement in Aqueous Solution for (ΔE_{aq}, in kcal/mol) for the Different Complexes Investigated in This Work: $CH_3NHCOCH_3...CH_3NHCOCH_3$ (I), $CH_3NHCOCH_3...CH_3NOHCOCH_3$ (II), $CH_3NHCOCH_3...CH_3OH$ (III), $CH_3NHCOMe...CH_3NNH_2COCH_3$ (IV), $CH_3NHCOMe...CH_3NH_2$ (V), and $CH_3NHCOCH_3...CH_3NHCSCH_3$ (VI)

complex	ΔG_{sol}	$\Delta\Delta G_{assoc}$	$E_{Int,aq}$	ΔE_{aq}
I	−16.4	1.8	−4.8	-
IIa	−14.6	4.7	−5.3	0.0
IIb	−18.2	1.8	−2.3	4.3
IIc	−15.2	3.9	−1.9	3.1
IIIa	−10.8	3.9	−2.1	0.0
IIIb	−13.0	1.7	−2.7	0.8
IVa	−12.8	7.9	−0.3	2.9
IVb	−15.7	4.4	−2.2	0.0
V	−9.29	4.4	0.6	-
VIa	−13.5	4.7	−3.5	2.1
VIb	−15.7	2.1	−2.7	0.0

[a] Free energies of solvation were computed at the PCM/6-311G(d,p) level using the geometries optimized in the gas phase at the MP2/6-31G(d) level.

Amide...Thioamide. Figure 8 shows the minimum-energy conformations of the bimolecular complexes $CH_3NHCOCH_3...CH_3NHCSCH_3$ (**VIa** and **VIb**). Complex **VIa** exhibits a hydrogen bond between the oxygen amide group and the hydrogen of the thioamide. It is 4.6 and 3.3 kcal/mol more stable than complex **VIb** at the HF/6-311G(d,p)//MP2/6-31G(d) and MP2/6-311G(d,p)//MP2/6-31G(d) levels, respectively, the latter being characterized by an interaction between the sulfur atom of the thioamide group and the hydrogen atom of the amide group. The relative stability of these complexes can be explained on the basis of the interaction and binding energies.

It is worth noting that complex **VIa** presents a binding energy of −7.4 kcal/mol, which is 1.5 kcal/mol more favorable than that predicted for complex **I**. This is a surprising result because the hydrogen atom of the thioamide group is less polar than the hydrogen atom of the amide group (Table 2). However, it can be noted that atomic charges are very small for all the atoms of the thioamide group with respect to those of the amide group. Accordingly, the repulsive contribution to the electrostatic term of the interaction energy is expected to be lower for **VIa** than that for **I**. On the other hand, the interaction and binding energies of complex **VIb** at the MP2/6-311G(d,p)//MP2/6-31G(d) level are −4.9 and −4.6 kcal/mol, respectively, indicating that the sulfur is a weaker hydrogen bond acceptor than oxygen.

Hydrogen-Bonding Interactions in the Aqueous Solution. In this section, the gas-phase results are compared with hydrogen bond formation in water. The free energies of solvation were computed for the 11 complexes under study using the PCM/6-311G(d,p) method. Geometries obtained from gas-phase optimizations at the MP2/6-31G(d) level were kept frozen during aqueous solution calculations. The ΔG_{sol} values predicted for the different complexes, which are displayed in Table 6, recall the favorable interaction with the solvent. Thus, ΔG_{sol} values range from −9.3 to −18.2 kcal/mol. A detailed analysis of the

results indicates that ΔG_{sol} decreases when the solvent-accessibility of the polar groups increases.

The difference between the free energy of solvation of the complex and the separated monomers ($\Delta\Delta G_{assoc}$ in Table 6) indicates that the hydrogen-bonding interactions are greatly modulated by the solvent and that the complexes are less solvated than their corresponding isolated monomers. The latter effect is mainly due to the dipole annihilation of the monomers in the complex and to the loss of hydrogen-bonding capabilities. The solvent-induced destabilization of complexes amounts to 1.8, 1.8−4.7, 4.4−7.9, and 2.1−4.7 kcal/mol for systems involving amide...amide, amide...*N*-hydroxamide, amide...*N*-amino amide, and amide...thioamide hydrogen-bonding interactions, respectively. Table 6 includes the interaction energies in aqueous solution (eq 4), which were computed considering the gas-phase interaction energies estimated at the MP2/6-311G-(d,p) level. As can be seen, even though the formation of complexes from the isolated monomers is not favored by the solvent, the interaction energy of all the complexes with exception of **V** is still favored in aqueous solution.

The energy difference in aqueous solution (ΔE_{aq} in Table 6) reveals that the environment plays an important contribution to the relative stability of the different arrangements within each complex. Thus, inspection to the results indicates that in general the preference for a given arrangement is largely reduced. For instance, complex **IIIa** is 3.1 kcal/mol favored with respect to **IIIb** in the gas phase, this energy difference being only 0.8 kcal/mol in the gas-phase. Complexes **IVa** and **IVb** are exceptions to this behavior. Thus, they are almost isoenergetic in the gas phase, whereas **IVb** is 2.9 kcal/mol favored with respect to **IVa** in aqueous solution.

Conclusions

This work provides an indication on the ability of the *N*-hydroxamide, *N*-amino amide, and thioamide groups to form hydrogen-bonding interactions in a peptide chain. The results indicate that the modified amide groups differ from the standard peptide bond not only in their local geometry but also in their hydrogen-bonding capabilities. The *N*-hydroxamide group is the strongest proton donor, being able to provide a strong binding with the carbonyl of the amide group. This interaction (complex **IIa**) is more favorable than the amide...amide one (complex **I**) by about 3 kcal/mol. On the other hand, the *N*-amino and thioamide groups are weaker proton donors than the *N*-hydroxamide group. However, the two groups present stronger proton-donating properties than the standard amide group. Moreover, the proton donor properties of the *N*-hydroxamide and *N*-amino amide groups are stronger than those of conventional hydroxyl and amino groups, respectively. The analysis of the proton acceptor properties reveals a similar behavior for the amide, *N*-hydroxamide, and *N*-amino amide groups. On the contrary, the thioamide group presents a weaker proton acceptor character, the binding energy associated with the thioamide-...amide hydrogen bond (complex **VIb**) being about 1 kcal/mol less favorable than that of the amide...amide interaction (complex **I**). SCRF calculations suggest that there is a poor tendency to form hydrogen-bonded complexes in aqueous solution. The results described in this work are useful for the design of new peptidomimetics.

Acknowledgment. C.A. thanks the Centre de Supercomputació de Catalunya (CESCA) for computational facilities.

References and Notes

(1) (a) Dauber-Osguthorpe, P.; Campbell, M. M.; Osguthorpe, D. J. *Int. J. Pept. Protein Res.* **1991**, *38*, 357. (b) Alemán, C.; Puiggalí, J. *J. Org. Chem.* **1995**, *60*, 910. (c) Benedetti, E.; Pedone, E. M.; Kawahata, N. H.; Gooman, M. *Biopolymers* **1995**, *36*, 659. (d)Alemán, C. *Proteins* **1997**, *29*, 575.

(2) (a) Chorev, M.; Shavitz, R.; Goodman, M.; Minick, S.; Guillemin, R. *Science* **1979**, *204*, 1210. (b) Verdini, A. S.; Silvestri, S.; Becherucci, C.; Longobardi, M. G.; Parente, L.; Peppoloni, S.; Perretti, M.; Pileri, P.; Pironi, M.; Viscomi; Nencioni, L. *J. Med. Chem.* **1991**, *34*, 3372. (c) Nishikawa, N.; Komazawa, H.; Orikasa, A.; Yoshikane, M.; Yamaguchi, J.; Kojima, M.; Ono, M.; Itoh, I.; Azuma, I.; Fujii, H.; Murata, J.; Saiki, I. *Bioorg. Med. Chem. Lett.* **1996**, *6*, 2725−2728. (d) Chorev, M.; Goodman, M. *Trends Biotechnol.* **1995**, *13*, 438−445.

(3) Spatola, A. F. In *Chemistry and Biochemistry of Amino Acids, Peptides and Proteins*; Weinstein, B., Ed; Marcel Dekker: New York, 1983; Vol. 7, pp 267−357.

(4) Marraud, M.; Dupont, V.; Grand, V.; Zerkout, S.; Lecoq, A.; Boussard, G.; Vidal, J.; Collet, A.; Aubry, A. *Biopolymers* **1993**, *33*, 1135.

(5) Dupont, V.; Lecoq, A.; Mangeot, J.-P.; Aubry, A.; Boussard, G.; Marraud, M. *J. Am. Chem. Soc.* **1993**, *115*, 8898−8906.

(6) (a) Hollósi, M.; Zewdu, F.; Kollát, E.; Majer, M.; Kajtár, M.; Batta, G.; Köver, K. E.; Sándor, P. *Int. J. Pept. Protein Res.* **1990**, *36*, 173. (b) Czugler, M.; Kálman, A.; Kajtár-Peredy, M.; Kollát, E.; Kajtár, J.; Majer, Z.; Farkas, Ö.; Hollósi, M. *Tetrahedrom* **1993**, *49*, 6661. (c) Shaw, R. A.; Kollát, E.; Hollósi, M.; Mantsch, H. H. *Spectrochim. Acta, Part A* **1995**, *51*, 1399. (d) Artis, D. R.; Lipton, M. A. *J. Am. Chem. Soc.* **1998**, *120*, 12200.

(7) (a) Jorgensen, W. L. *J. Am. Chem. Soc.* **1989**, *111*, 3770. (b) Sneddon, S. F.; Tobias, D. J.; Brooks, C. L. III *J. Mol. Biol.* **1989**, *209*, 817. (c) Cieplak, P.; Kollman, P. A. *J. Comput. Chem.* **1991**, *112*, 1232. (d) Luque, F. J.; Orozco, M. *J. Org. Chem.* **1993**, *58*, 6397. (e) Simonson, T.; Brunger, A. T. *J. Phys. Chem.* **1994**, *98*, 4683. (f) Guo, H.; Karplus, M. *J. Phys. Chem.* **1994**, *98*, 7104. (g) Ösapay, K.; Young, W. S.; Bashford, D.; Brooks, C. L.; Case, D. *J. Phys. Chem.* **1996**, *100*, 2698. (h) Ben-Tal, N.; Stikoff, D.; Topol, I. A.; Yang, A. S.; Burt, S. K.; Honig, B. *J. Phys. Chem. B* **1997**, *101*, 450.

(8) Frisch, M. J.; Trucks, G. W.; Schlegel, H. B.; Scuseria, G. E.; Robb, M. A.; Cheeseman, J. R.; Zakrzewski, V. G.; Montgomery, Jr.; Stratmann, R. E.; Burant, J. C.; Dapprich, S.; Millam, J. M.; Daniels, A. D.; Kudin, K. N.; Strain, M. C.; Farkas, O.; Tomasi, J.; Barone, V.; Cossi, M.; Cammi, R.; Mennucci, B.; Pomelli, C.; Adamo, C.; Clifford, S.; Ochterski, J.; Petersson, G. A.; Ayala, P. Y.; Cui, Q.; Morokuma, K.; Malick, D. K.; Rabuck, A. D.; Raghavachari, K.; Foresman, J. B.; Cioslowski, J.; Ortiz, J. V.; Baboul, A. G.; Stefanov, B. B.; Liu, G.; Liashenko, A.; Piskorz, P.; Komaromi, I.; Gomperts, R.; Martin, R. L.; Fox, D. J.; Keith, T.; Al-Laham, M. A.; Peng, C. Y.; Nanayakkara, A.; Gonzalez, C.; Challacombe, M.; Gill, P. M. W.; Johnson, B.; Chen, W.; Wong, M. W.; Andres, J. L.; Gonzalez, C.; Head-Gordon, M.; Replogle, E. S.; Pople, J. A. *Gaussian 98*, Revision A.7; Gaussian, Inc.: Pittsburgh, PA, 1998.

(9) Møller, C.; Plesset, M. S. *Phys. Rev.* **1934**, *46*, 618.

(10) Hariharan, P. C.; Pople, J. A. *Theor. Chim. Acta* **1973**, *23*, 213.

(11) Frisch, M. J.; Pople, J. A.; Binkley, J. S. *J. Chem. Phys.* **1984**, *80*, 3265.

(12) Boys, S. F.; Bernardi, F. *Mol. Phys.* **1970**, *19*, 553.

(13) Miertus, S.; Scrocco, E.; Tomasi, J. *Chem. Phys.* **1981**, *55*, 117.

(14) Hawkins, G. D.; Cramer, C. J.; Truhlar, D. G. *J. Phys. Chem. B* **1998**, *102*, 3257.

(15) Besler, B. H.; Mertz, K. M.; Kollman, P. A. *J. Comput. Chem.* **1990**, *11*, 431.

(16) (a) Novoa, J. J.; Planas, M.; Whangbo, M.-H. *Chem. Phys. Lett.* **1994**, *225*, 240. (b) Gutowski, M.; van Duijneveldt-van de Rijdt, J. G.; C. M.; van Lenthe, J. H.; van Duijneveldt, F. B. *J. Chem. Phys.* **1993**, *98*, 4728.

(17) (a) Zheng, Y. J.; Merz, K. M. *J. Comput Chem* **1992**, *13*, 1152. (b) Colominas, C.; Teixidó, J.; Cemelí, J.; Luque, F. J.; Orozco, M. *J. Phys. Chem. B* **1998**, *102*, 2269.